58

ИНСТИТУТ ЯДЕРНОЙ ФИЗИКИ СО АН СССР

A. Gerasimov, F.M. Izrailev, J.L. Tennyson,
A.B. Temnykh

THE DYNAMICS OF THE BEAM-BEAM INTERACTION

PREPRINT 86-100

НОВОСИБИРСК
1986

THE DYNAMICS OF THE BEAM-BEAM INTERACTION

A. Gerasimov, F.M. Izrailev, J.L. Tennyson, A.B. Temnykh

Institute of Nuclear Physics
630090, Novosibirsk 90, USSR

Abstract

The beam-beam interaction is responsible for loss of luminosity and beam lifetime in colliding beams machines. In this work, the properties of nonlinear beam-beam resonances in the full three-degrees-of-freedom system are examined. Theoretical conjectures concerning the mechanisms for luminosity and lifetime degradation are compared with the results of simulation and experimentation at VEP-4. It is shown that machine nonlinearity may also play an important role in limiting the lifetime.

I. INTRODUCTION

In a colliding-beam storage ring, the beam-beam interaction is the collective, relativistically enhanced, transverse electromagnetic force experienced by a beam particle as it passes through a bunch of the opposing beam.

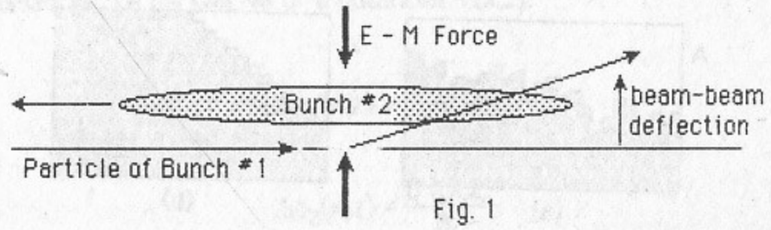

Fig. 1

Every time a particle of one beam passes through a bunch of the opposing beam, it experiences a transverse kick which changes the amplitude of its vertical and horizontal betatron oscillation.

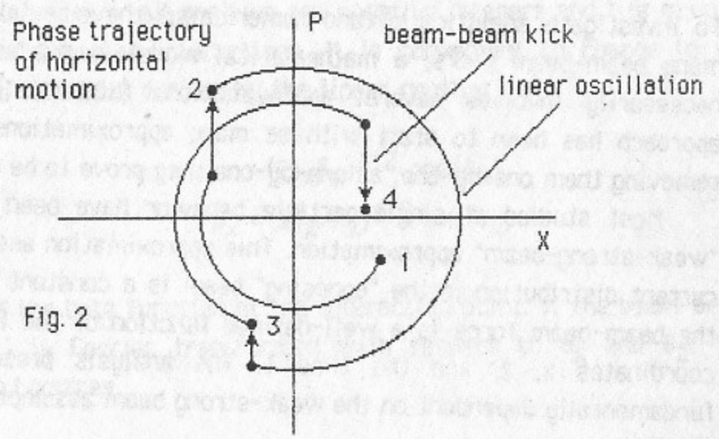

Fig. 2

The beam-beam kicks are important because they can cause the amplitudes of both the vertical and horizontal betatron oscillations to increase, either via diffusion caused by a sequence of uncorrelated kicks, or via resonant pumping caused by a sequence of highly correlated kicks. This growth of betatron amplitudes can cause loss of luminosity and/or beam lifetime.

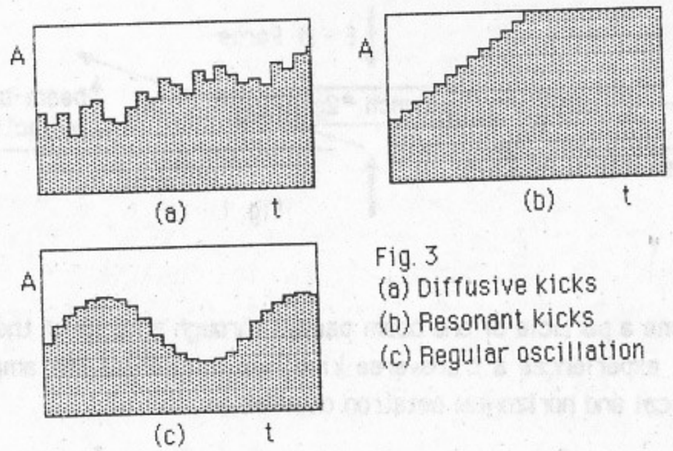

Fig. 3
(a) Diffusive kicks
(b) Resonant kicks
(c) Regular oscillation

To investigate analytically (and numerically) the cumulative effect of many beam-beam kicks, a mathematical model is needed. This model necessarily involves several approximations (historically, the usual approach has been to start with as many approximations as possible, removing them one-by-one, as one-by-one they prove to be unrealistic).

Most studies of single particle behavior have been based on the "weak-strong-beam" approximation. This approximation assumes that the current distribution in the "opposing" beam is a constant and thus, that the beam-beam force is a well-defined function of the two transverse coordinates x, z, and the time t. The analysis presented here is fundamentally dependent on the weak-strong beam assumption.

II. THE HAMILTONIAN

The simplest two dimensional model of the colliding beam system consists of two linear oscillators and a periodic kick which changes instantly the two momenta. The oscillators are coupled since the beam-beam kick for each oscillator depends not only on its own coordinate, but on the coordinate of the other oscillator as well $\Delta p_x(x,z)$, $\Delta p_z(x,z)$. The magnitude of the beam-beam kick may be expressed as the derivative of a potential $V(x,z)$.

$$\Delta p_x(x,z) = \frac{\partial V(x,z)}{\partial x} \qquad (1)$$
$$\Delta p_z(x,z) = \frac{\partial V(x,z)}{\partial z}$$

The system as a whole may be roughly represented (less the damping and quantum fluctuations) by the Hamiltonian

$$H = H_v(z,p_z) + H_h(x,p_x) + \sum_n \delta(t-n)\, V(x,z) \qquad (2)$$

where the sum is over all positive and negative integers and t is in units of the period between interactions. It is convenient to change to the action-angle variables defined by the linear oscillations

$$x = (2I_x\beta_x)^{1/2} \cos(\theta_x)$$
$$p_x = (2I_x/\beta_x)^{1/2} \sin(\theta_x) \qquad (3)$$

where β_x is the beta function at the interaction point. If the beam-beam term in (2) is Fourier transformed with respect to θ_x and θ_z, the Hamiltonian becomes

$$H = I_x\Omega_x + I_z\Omega_z + \sum_n \sum_{m_x} \sum_{m_z} F_{\underline{m}}(\underline{I}) \cos(m_x\theta_x + m_z\theta_z + 2\pi nt) \quad (4)$$

The $\underline{m}$=0 term is independent of θ_x and θ_z. It is convenient to define an integrable nonlinear oscillator $H_0(\underline{I})$ by adding together the two linear oscillator terms and the $\underline{m}$=0 term from the perturbation expansion. Equation (4) then becomes

$$H = H_0(\underline{I}) + \sum_n \sum_{\substack{\underline{m} \\ \underline{m}\neq 0}} F_{\underline{m}}(\underline{I}) \cos(m_x\theta_x + m_z\theta_z + 2\pi nt) \quad (5)$$

This Hamiltonian does not correspond to an integrable system, but a finite portion of its phase space is covered by regular trajectories, i.e. trajectories that are bounded for all time and are characterized by discrete frequency spectra (of phase variables). The behavior of such a system is very complicated and can only be understood by carefully examining the properties of its nonlinear resonances (represented by the Fourier terms of (5)).

An analysis of a certain nonlinear resonance $\underline{m}$ usually assumes that all of the other Fourier terms in (5) can be neglected. The resonance Hamiltonian is then

$$H_{\underline{m}} = H_0(\underline{I}) + F_{\underline{m}}(\underline{I}) \cos(m_x\theta_x + m_z\theta_z + 2\pi nt) \quad (6)$$

The time derivative of the action from Hamilton's equations is

$$\dot{\underline{I}} = -\frac{\partial H_{\underline{m}}}{\partial \underline{\theta}} = \underline{m}\, F_{\underline{m}}(\underline{I}) \sin(m_x\theta_x + m_z\theta_z + 2\pi nt) \quad (7)$$

Thus, in the action space (I_x, I_z), the motion defined by the Hamiltonian (6) lies on a line parallel to the vector $\underline{m}$. The frequency of oscillation in action space is determined by the time rate of change $d\psi_{\underline{m}}/dt$ of the resonance phase

$$\psi_{\underline{m}} = m_x\theta_x + m_z\theta_z + 2\pi nt \quad (8)$$

The resonance system (6) is said to be "in resonance" if $d\psi_{\underline{m}}/dt = 0$, i.e. if

$$m_x\dot{\theta}_x + m_z\dot{\theta}_z + 2\pi n = 0 \quad (9)$$

The frequencies $\dot{\theta}_x$ and $\dot{\theta}_z$ are, to zero order, determined by H_0

$$\dot{\theta}_x \approx \omega_x(\underline{I}) \equiv \frac{\partial H_0(\underline{I})}{\partial I_x}$$
$$\dot{\theta}_z \approx \omega_z(\underline{I}) \equiv \frac{\partial H_0(\underline{I})}{\partial I_z} \quad (10)$$

and are functions of the actions I_x and I_z. Thus, the resonance condition (9) defines a line in the action space. The resonance line and the direction of resonance oscillation are illustrated in Fig. 4.

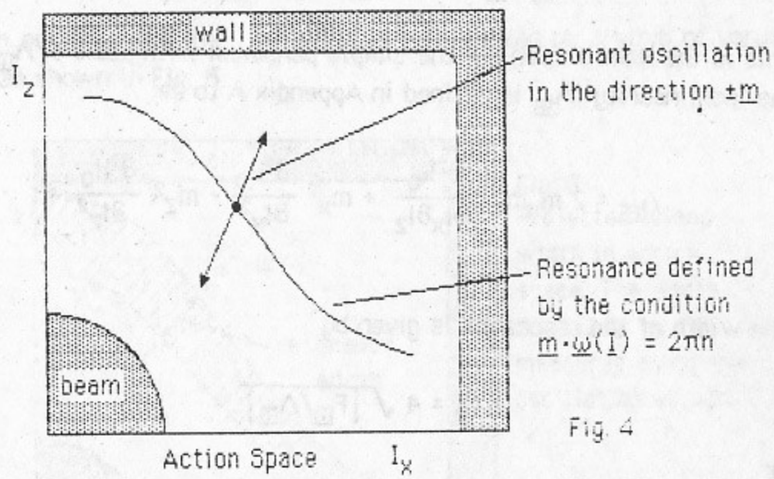

Fig. 4

III. RESONANCE CHARACTERISTICS

Besides its location and the direction of its resonant oscillation, the nonlinear resonance is characterized by its width in action space and its frequency of small amplitude oscillation. By transforming to the resonance phase $\psi_{\underline{m}}$ and its corresponding conjugate momentum $I_{\underline{m}}$, it's possible to reduce the system to one degree of freedom. Taylor expanding the zero order Hamiltonian H_0 about some point $\underline{I}_0$ which satisfies

$$m_x\omega_x(\underline{I}_0) + m_z\omega_z(\underline{I}_0) + 2\pi n = 0 \qquad (11)$$

i.e. which is on the resonance curve in action space, and with

$$\psi_{\underline{m}} = m_x\theta_x + m_z\theta_z + 2\pi nt \qquad (12)$$

the Hamiltonian for the resonance is given by (see Appendix A for details)

$$H(I_{\underline{m}},\psi_{\underline{m}}) = 1/2\ \ I_{\underline{m}}^2\,\Lambda_{\underline{m}} + F_{\underline{m}}(\underline{I}_0)\cos\psi_{\underline{m}} \qquad (13)$$

This is the Hamiltonian for the simple pendulum with mass $1/\Lambda_{\underline{m}}$, where the "nonlinearity" $\Lambda_{\underline{m}}$ is defined in Appendix A to be

$$\Lambda_{\underline{m}} = 2\,m_x m_z \frac{\partial^2 H_0}{\partial I_x \partial I_z} + m_x^2 \frac{\partial^2 H_0}{\partial I_x^2} + m_z^2 \frac{\partial^2 H_0}{\partial I_z^2} \qquad (14)$$

The width of the resonance is given by

$$\Delta I_{\underline{m}} = 4\sqrt{\left|F_{\underline{m}}/\Lambda_{\underline{m}}\right|} \qquad (15)$$

or

$$\Delta\underline{I} = \underline{m}\,\Delta I_{\underline{m}} \qquad (16)$$

while the frequency of small amplitude oscillation is

$$\omega_{\underline{m}} = \sqrt{\left|F_{\underline{m}}\,\Lambda_{\underline{m}}\right|} \qquad (17)$$

The phase portrait of the nonlinear resonance is shown in Fig. 5.

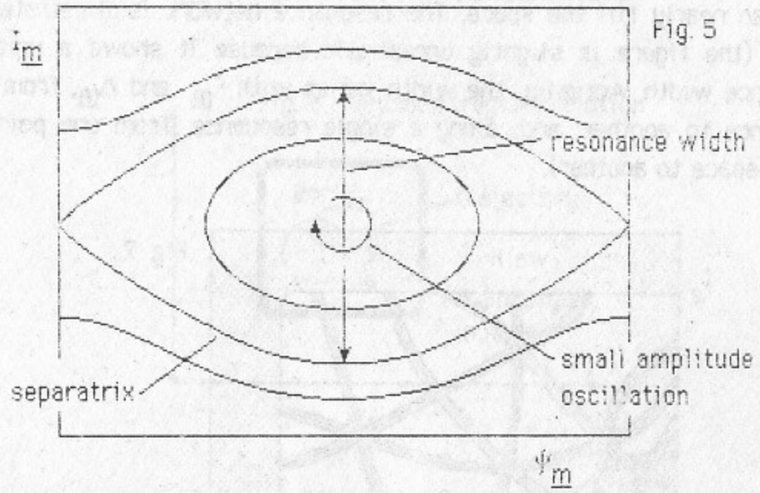

Fig. 5

Thus, in action space, the resonance is represented by a strip of varying width, as shown in Fig. 6.

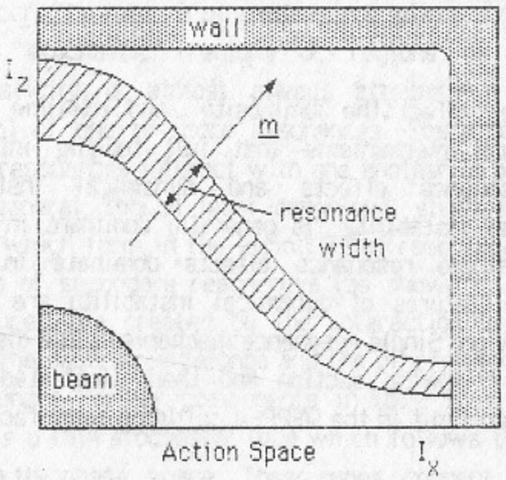

Fig. 6
Projected island width in action space. The width ΔI_x, ΔI_z is measured along the oscillation vector.

If all of the resonance curves could be plotted in the action space, they would form a dense network of intersecting paths. Although the resonances each have a finite width and are dense, they do not fill the space (the measure of nonresonant points is non-zero). However, if the resonance widths are larger than the typical spacings between them, they can nearly fill the space. The resonance network is illustrated in Fig. 7 (the figure is slightly unrealistic because it shows a uniform resonance width. Actually, the widtn varies with $F_{\underline{m}}$ and $\Lambda_{\underline{m}}$, from one resonance to another, and, along a single resonance, from one point in action space to another).

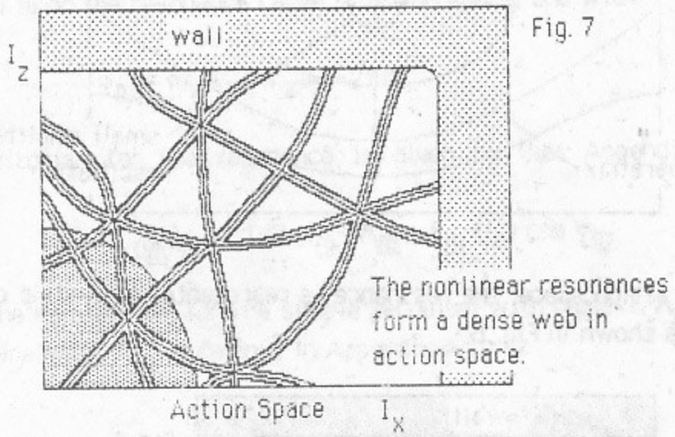

Fig. 7

How do these resonances affect the luminosity and lifetime of the beam? There are several mechanisms that fall roughly into two catagories: single resonance effects and dynamical instability (stochasticity). Dynamical instability is generally dominant in hadron storage rings, while single resonance effects dominate in e^+-e^- colliders. The principal features of dynamical instability are briefly reviewed in the next section. Single resonance mechanisms are discussed in more detail in the following section and then illustrated in an analysis of the beam-beam limit in the VEPP-4 colliding beam facility at Novosibirsk.

IV. DYNAMICAL INSTABILITY

It can be proved (the "KAM" theorem) that although nonresonant particles oscillate slightly in the action space due to the beam-beam interaction, they are confined eternally (for the ideal Hamiltonian system (2)) to a neighborhood of their initial conditions

Fig. 8 Bounded (regular) motion

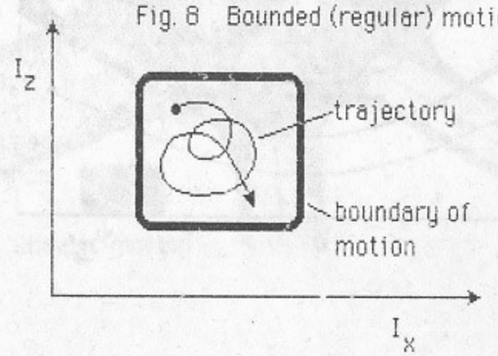

Consecutive kicks from the beam-beam interaction are perfectly correlated so that no diffusion takes place. But when particles are close to a resonance in action space, correlations can break down and diffusion can occur. The regions of phase space where correlations break down are called "stochastic" regions or regions of "dynamical instability". Stochasticity is almost always attributable to the interaction (or overlap) of one or more resonances. There are several situations in which resonances interact with one another to produce stochasticity. The most general, though least dangerous, stochastic regions are the thin layers which form in the vicinities of resonance separatrices due to the overlap of secondary resonances (as shown in Fig. 9). These secondary resonances are created by the interaction between the resonance to which the separatrix belongs and the other resonances in the system (the nonresonant Fourier components in (6)). Thus, around every resonance there is a thin stochastic tube which follows the resonance wherever it goes in the phase space. These tubes connect with each other at the

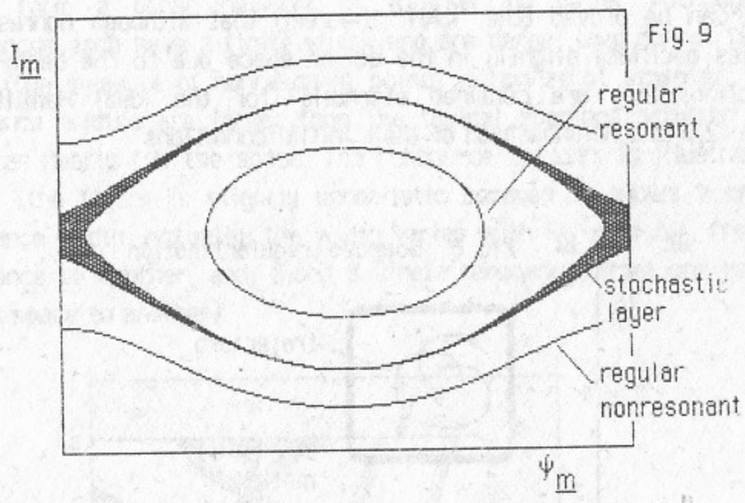

Fig. 9

resonance intersections (see Fig. 7). Since the resonances are dense in the phase space, a particle starting inside any stochastic layer can eventually diffuse into any other region of phase space. This universal diffusion is called "Arnold diffusion" (for a detailed description of the thin stochastic layer and Arnold diffusion, see Chirikov [1]). Since Arnold diffusion is very slow, and effects only a tiny portion of the phase space, it is usually negligible in comparison to other beam-beam effects.

Another area where stochasticity occurs is at the intersections of the resonances in phase space. The stochasticity in these areas is much stronger than the thin-layer stochasticity, but since the intersections are relatively isolated (except for the thin-layer bridges that connect them), they are not dangerous unless they are very large. A rough illustration of a resonance intersection and the accompanying stochastic region are shown in Fig. 10.

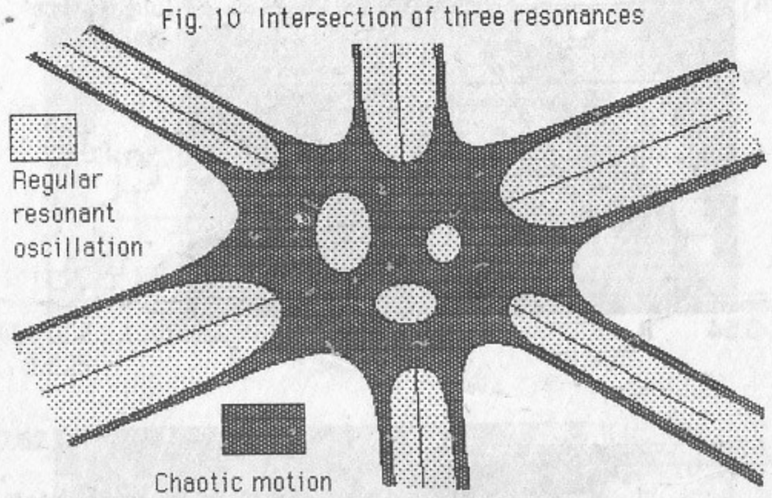

Fig. 10 Intersection of three resonances

V. STUDIES AT VEPP-4

The VEPP-4 colliding beams machine in Novosibirsk operates at a maximum energy of 5.1 GeV with luminosity 5×10^{30} and a minimum beam lifetime of 3 hours. The tune shifts are approximately ξ_z=.06 and ξ_x=.02 with typical working tunes at υ_x=8.535 and υ_z=9.585. The synchrotron tune is about υ_y=.02 and the vertical tune variation due to the longitudinal synchrotron oscillation is about $\Delta\upsilon_y$=.015 at a synchrotron oscillation amplitude of $A_y=\sigma_y$. There is only one interaction point. An electrostatic deflector separates the beam on the other side of the ring.

Measurements were recently made (A. Temnykh [2]) of the machine's luminosity and lifetime over a wide range of working tunes. The results of these measurements are shown in Fig.s 11 and 12.

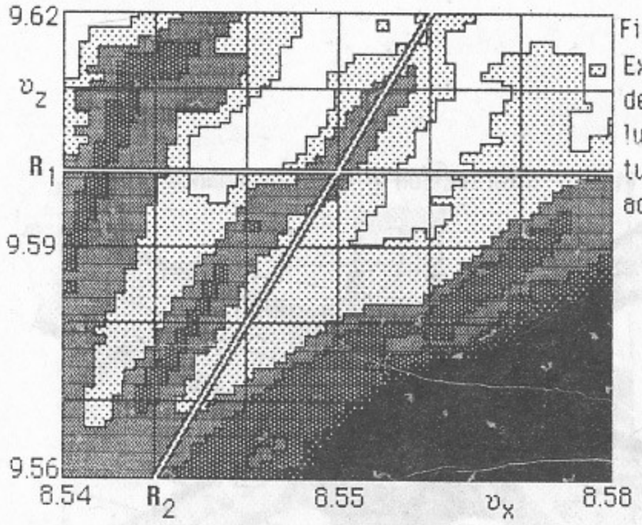

Fig. 11a
Experimental dependence of luminosity on tune; before adjustment.

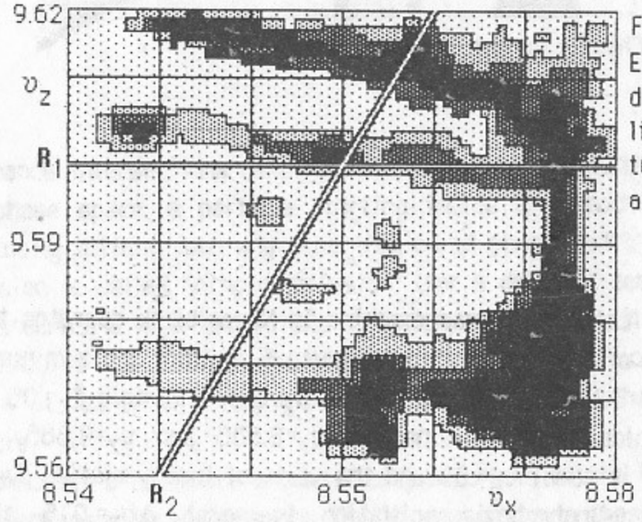

Fig. 11b
Experimental dependence of lifetime on tune; before adjustment.

Two sets of data were collected, one of them, Fig.11, before an adjustment of the lattice configuration in September 1984, and the other, Fig. 12, after the adjustment (it is thought that the machine nonlinearity changed sign during this adjustment, from positive to

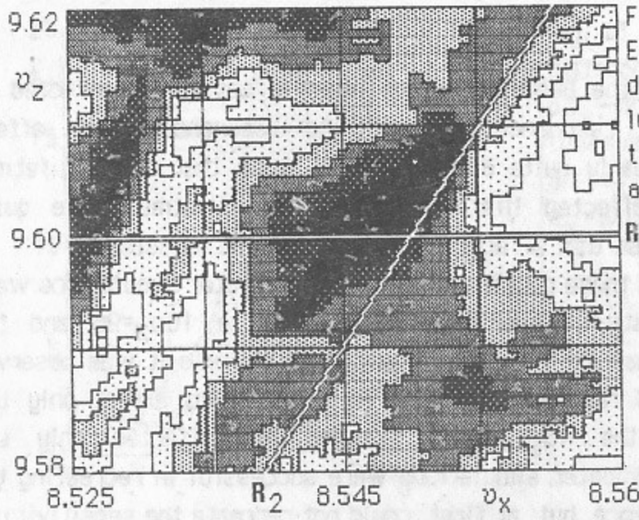

Fig. 12a
Experimental dependence of luminosity on tune; after adjustment.

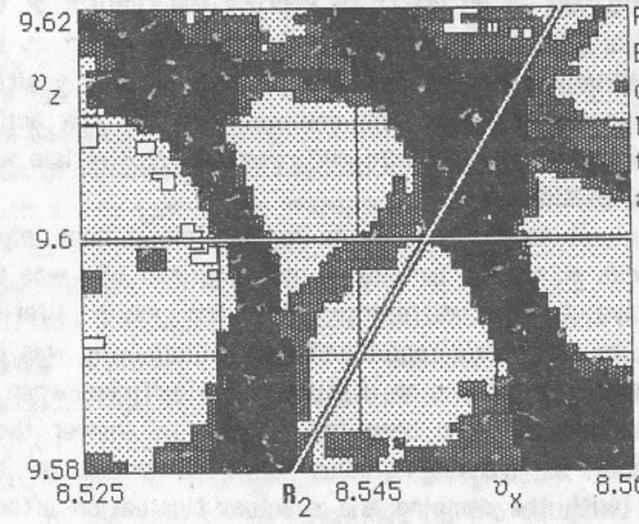

Fig. 12b
Expertimental dependence of lifetime on tune; after adjustment.

negative. "Positive" refers to the case where the machine tune shift is positive). The darker the shading in these figures, the poorer the performance. In some of these plots (primarily in Fig. 11a), there is an artificial shear displacement of the contours along the left-to-right diagonal. This defect was apparently caused by hysteresis when the time derivative of the magnetic field changed sign during the automated tune scan.

In all four plots, the behavior of the beam is apparently affected by certain nonlinear resonances, though the resonances that affect luminosity are clearly quite different from those that affect lifetime and those that affected lifetime before the adjustment are quite different from those that affected lifetime after the adjustment.

To understand these results, a number of computer simulations were run in the vicinity of the intersections of the $10\upsilon_z=96$ and the $4\upsilon_x-2\upsilon_z=15$ resonances. This area was chosen because it was observed that the $10\upsilon_z=96$ resonance (labeled R_1) seemed to affect only the lifetime, while the $4\upsilon_x-2\upsilon_z=15$ (labeled R_2) affected only the luminosity. The computer simulations were successful in recreating the luminosity dependence, but, at first, could not recreate the sensitivity of lifetime to the $10\upsilon_z=96$. In an effort to improve the realism of the simulation model, a thin nonlinear (octupole) lens was added at the interaction point. With the lens (whose strength was set to a positive value comparable in magnitude to the octupole error in the actual machine), the adverse effect of the $10\upsilon_z=96$ resonance on lifetime was clearly observed in the simulation.

The next step was to investigate the mechanisms through which these two resonances affect the luminosity and lifetime. Why was the luminosity sensitive to the difference resonance while lifetime responded only to the parametric resonance? Furthermore, why was the effect of the parametric resonance on lifetime only significant when an octupole field was added to the beam-beam kick? To answer these questions, a number of tracking studies were performed on the simulation model (with the damping and quantum fluctuation effects removed). Surface-of-section plots were made in order to observe the location, width, and oscillation direction of the two resonances. The results of these "tracking" studies are shown in Fig.s 13-14. These studies were quite successful in explaining the results of the simulation, and (presumably) the sensitivity of the actual machine to these resonances.

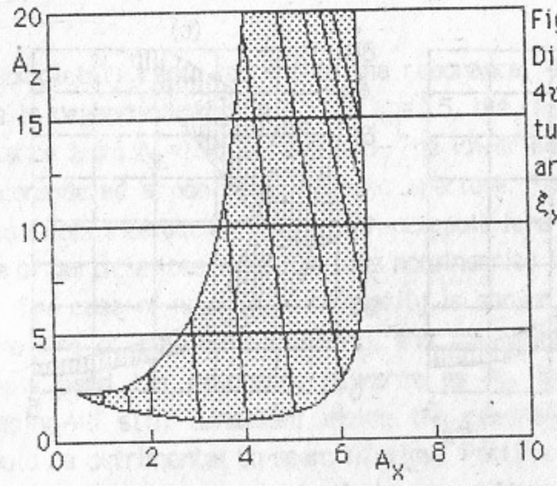

Fig. 13
Difference resonance $4\upsilon_x - 2\upsilon_z = 15$. The tunes and tune shifts are υ_x =.550 υ_z =.601 ξ_x =.01, ξ_z =.03.

In Fig. 13 it is clearly seen that the difference resonance $4\upsilon_x-2\upsilon_z=15$ is very large, even at relatively small amplitudes, and that its nearly vertical resonant oscillation can easily move particles out of the beam core, resulting in a blow up of the beam and an accompanying loss of luminosity. The resonant oscillation is not, however, situated in such a way that it can transport particles all the way to the aperture (which is located approximately at $A_z=80\sigma_z$); its oscillation does not span sufficiently large intervals of A_z when $A_x \leq 5\sigma_x$.

The parametric resonance $10\upsilon_z=96$ is shown in Fig. 14. The three cases correspond to zero, positive, and negative nonlinearity, respectively. All three were calculated at υ_z=.599, υ_x=.555, ξ_z=.03, ξ_x=.01. The magnitudes of the octupole-induced tune shifts were $\Delta\upsilon_x=\pm 2.5 \times 10^{-5}$ at $A_z=0$, $A_x=1$ and $\Delta\upsilon_z=\pm 2.5 \times 10^{-7}$ at $A_z=1$, $A_x=0$.

In the case of zero nonlinearity (no octupole lens) the resonance spans the distance from about $A_z=20\sigma_z$ to $A_z=40\sigma_z$ at $A_x=0$. The period of resonant oscillation is about 20% of the damping time. The direction of resonant oscillation is vertical, so that vertical damping is eliminated inside the resonance.

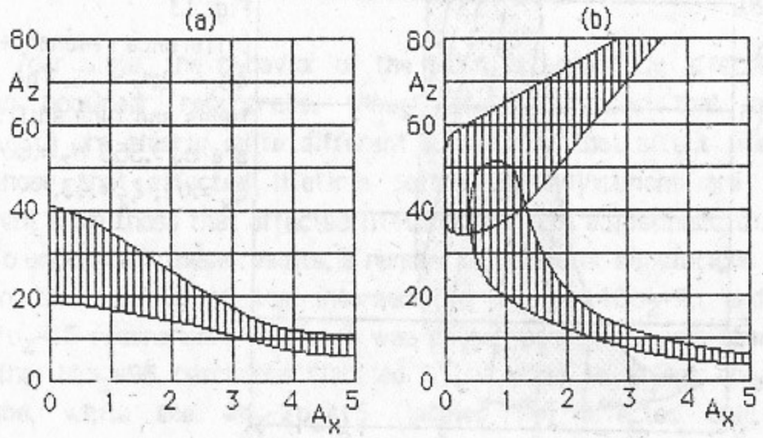

Fig. 14 Projection of $10\upsilon_z = 96$ onto the amplitude plane for the cases of (a) zero nonlinearity, (b) positive nonlinearity, and (c) negative nonlinearity. The tunes here are $\upsilon_x = .555$, $\upsilon_z = .559$, the tune shifts $\xi_x = .01$, $\xi_z = .03$. The machine-nonlinear tune shift at $A_x = 0$, $A_z = 1$ is $\Delta\upsilon_z = 2.5 \times 10^{-7}$ and at $A_z = 0$, $A_x = 1$ is $\Delta\upsilon_x = 2.5 \times 10^{-5}$.

It is therefore expected that at small x amplitudes, the density of particles between $A_z=20\sigma_z$ and $A_z=40\sigma_z$ is approximately constant. However, the aperture is at about 80σ, and without additional resonances, it is very difficult for a particle to overcome the very strong damping between $40\sigma_z$ and $80\sigma_z$. The situation changes dramatically (as shown by Temnykh in Ref. 3) when positive nonlinearity is added (Fig. 14b). On a certain line in amplitude space, the beam-beam induced nonlinearity is cancelled by the octupole induced nonlinearity. Where the resonance crosses this line, it folds back on itself and a region of very wide oscillation appears. Since a sufficiently small vertical damping

is completely cancelled inside the resonance, the particle distribution here is dependent only on A_x. At $A_x=1.5$, the resonance spans the entire distance from $A_z=15\sigma$ to $A_z=70\sigma$. The lower edge of the resonance can be considered a nonlinear dynamic aperture. Thus, the coupling of the beam-beam interaction with a thin octupole lens can seriously affect the rate of particle loss when the lens nonlinearity is positive.

The case of negative nonlinearity is shown in Fig. 14c. Here there is no line of zero z-nonlinearity, and the effect of the octupole is to simply bend the resonance upwards as A_x increases. Since vertical damping is still cancelled inside the resonance, even this situation should be detrimental to beam lifetime. Particles entering the resonance at its bottom edge should be able to diffuse (from quantum-induced fluctuations of A_x) up the resonance to the aperture. However, since the area covered by the resonance is much smaller here than in the previous case, the reduction in lifetime is also expected to be smaller.

Figures 13 and 14 were drawn using numerically generated surface-of-section plots of particle orbits in P_z, z phase space. Two examples are shown in Fig. 15. The first shows resonant tori in the "fold" region of Fig. 14b.

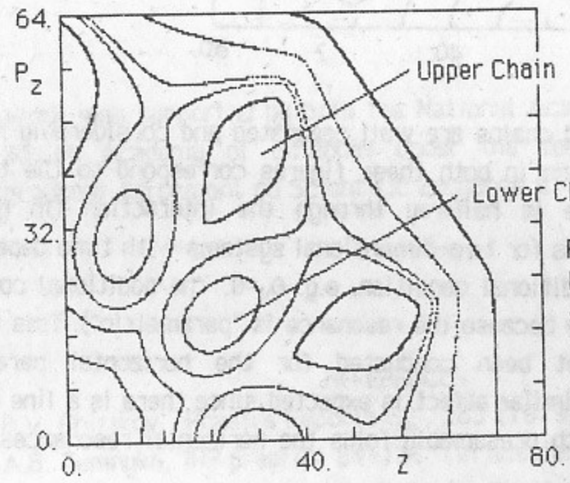

Fig. 15a Phase space section of Fig 14b taken at $A_x = .95$.

The section is taken at A_x=1. Two separate island chains of unusually large width are interwoven. Both chains are manifestations of the same resonance $10\upsilon_z$=96. One chain lies above the line of zero nonlinearity, the other below. Note that although these two chains overlap in the amplitude space projection (this is shown explicitly in Fig.14b) they are out of phase and so do not overlap in phase space (there is no significant stochasticity in this area). Figure 15b shows a phase plane section at a larger x amplitude A_x=1.5.

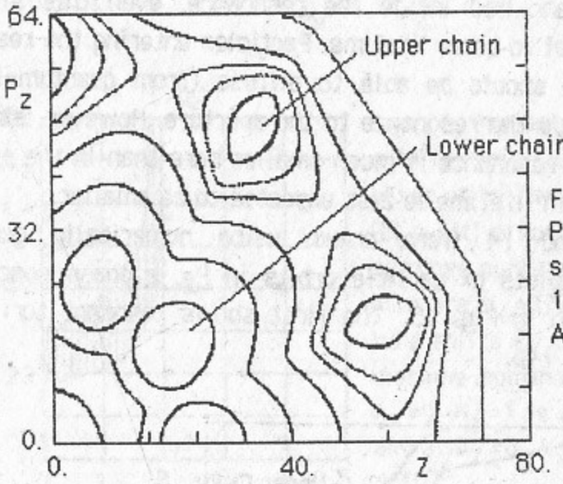

Fig. 15b
Phase space section of Fig. 14b, taken at A_x =1.5.

Here the two island chains are well separated and considerably reduced in size. The sections in both these figures correspond to the time at which the particle is halfway through the interaction (in general, phase-space sections for two-dimensional systems with time dependence must satisfy an additional condition, e.g. θ_x=0. The additional condition is not required here because the resonance is "parametric"). This type of study has not yet been conducted for the horizontal parametric resonances, but a similar effect is expected since there is a line of zero x-nonlinearity which presumably folds the horizontal resonances in the same way.

The sign of the machine-induced nonlinearity in the experiment Fig.11 is not known, though it is thought to have been positive. However, it was fairly well established that the nonlinearity in the later experiments Fig.12 was negative. In the earlier experiments, the prominence of the difference resonances in the luminosity measurements, and (if the nonlinearity was really positive) the prominence of the parametric resonances in the lifetime measurements, can be (qualitatively) explained by the above mechanisms. In the later luminosity measurement, the difference resonances are not as distinct, but remain the dominant recognizable features. Machine nonlinearity is not expected to have a sizable effect on luminosity since its strengths at small amplitudes is small compared to that of the beam-beam interaction. However, the later measurement of lifetime contrasts rather drastically with the earlier measurement. Careful surface-of-section studies have not yet been completed, but preliminary investigations have thus far not been successful in identifying the extremely influential sum resonances which appear in Fig. 12b (there is some indication that they may be odd-order resonances resulting from a slight misallignment of the beam centers).

This work was supported by both the National Academy of Sciences and the Soviet Academy of Sciences under the terms of the US-USSR interacademy Agreement on Scientific Exchange and Cooperation.

REFERENCES

1. B.V. Chirikov, Physics Reports 52 , 263 (1979).
2. A.B. Temnykh, INP preprint 84-131 (in Russian).
3. A.B. Temnykh, INP preprint 84-143 (in Russian).

APPENDIX A Resonance Hamiltonian

The resonance Hamiltonian (6) includes only one Fourier term of the full interaction energy

$$H_{\underline{m}} = H_0(\underline{I}) + F_{\underline{m}}(\underline{I}) \cos (m_x\theta_x + m_z\theta_z + 2\pi nt) \qquad (A1)$$

This may be approximated in the vicinity of some phase point $\underline{I}_0$ by fixing $F_{\underline{m}}(\underline{I})$ at its value at $\underline{I}_0$ and replacing $H_0(\underline{I})$ by the first two terms of its Taylor series expansion about $\underline{I}_0$

$$H_{\underline{m}} \approx H_0(\underline{I}_0) + \underline{\omega}_0\cdot\Delta\underline{I} + 1/2\ \Delta\underline{I}\cdot\frac{\partial\underline{\omega}}{\partial\underline{I}}\cdot\Delta\underline{I} + F_{\underline{m}}(\underline{I}_0)\cos(\ldots) \qquad (A2)$$

where $\underline{\omega}_0 \equiv \partial H_0/\partial\underline{I}$, and $\Delta\underline{I} \equiv \underline{I} - \underline{I}_0$. The Hamiltonian (A2) is integrable and may be expressed in terms of a single pair of conjugate coordinates $(I_{\underline{m}},\psi_{\underline{m}})$. The generating function is

$$G = \underline{I}_0\cdot\underline{\theta} - I_{\underline{m}}\,(m_x\theta_x + m_z\theta_z + 2\pi nt) \qquad (A3)$$

Then with

$$\psi_{\underline{m}} = (m_x\theta_x + m_z\theta_z + 2\pi nt) \qquad (A4)$$

$$\Delta I_x = I_{\underline{m}}\, m_x$$
$$\Delta I_z = I_{\underline{m}}\, m_z$$

equation (A2) becomes

$$H_{\underline{m}} \approx H_0(\underline{I}) + (\underline{\omega}_0\cdot\underline{m} + 2\pi n)\, I_{\underline{m}} + 1/2\ I_{\underline{m}}^2\,[\,\underline{m}\cdot\frac{\partial\underline{\omega}}{\partial\underline{I}}\cdot\underline{m}\,] + F_{\underline{m}}(\underline{I}_0)\cos\psi_{\underline{m}} \qquad (A5)$$

If $\underline{I}_0$ is chosen such that it lies on the resonance line, i.e.

$$m_x\omega_x(\underline{I}_0) + m_z\omega_z(\underline{I}_0) + 2\pi n = 0$$

then the second term in (A5) is zero and the first term is constant (and can be dropped). Thus

$$H_{\underline{m}}(I_{\underline{m}},\psi_{\underline{m}}) = 1/2\ I_{\underline{m}}^2\,[\,\underline{m}\cdot\frac{\partial\underline{\omega}}{\partial\underline{I}}\cdot\underline{m}\,] + F_{\underline{m}}(\underline{I}_0)\cos\psi_{\underline{m}} \qquad (A6)$$

Defining

$$\Lambda_{\underline{m}} = 2\,m_x m_z\,\frac{\partial^2 H_0}{\partial I_x \partial I_z} + m_x^2\,\frac{\partial^2 H_0}{\partial I_x^2} + m_z^2\,\frac{\partial^2 H_0}{\partial I_z^2} \qquad (A7)$$

the resonance Hamiltonian (A6) becomes

$$H_{\underline{m}}(I_{\underline{m}},\psi_{\underline{m}}) = 1/2\ I_{\underline{m}}^2\,\Lambda_{\underline{m}} + F_{\underline{m}}(\underline{I}_0)\cos\psi_{\underline{m}} \qquad (A8)$$

This is a pendulum with separatrix width

$$\Delta I_{\underline{m}} = 4\,\sqrt{|F_{\underline{m}}/\Lambda_{\underline{m}}|} \qquad (A9)$$

or, from (A4)

$$\Delta I_x = |m_x \Delta I_{\underline{m}}|$$
$$\Delta I_z = |m_z \Delta I_{\underline{m}}| \qquad \text{(A10)}$$

APPENDIX B Beam Beam Model and Simulation

The simulation model features

a) Two transverse and one longitudinal oscillations
b) Accurate analytic 2-D beam-beam kick
c) Linear phase advance between interactions
d) Damping and quantum fluctuations in all three oscillations
e) Small vertical tune variation at interaction point
f) Thin octupole lens at interaction point

The beam-beam kick is given by a potential

$$\varphi = \frac{A}{f(z) + g(x)} - F \ln [\, h(z,x) \,] \qquad \text{(B1)}$$

where $f(z) = \sqrt{z^2 + B} + Cz^2$

$g(x) = D \exp(+x^2/E)$

$h(z,x) = (x^2 + z^2 + G)$

where A=11.48 B=2. (σ_z/σ_x) C=.6
D=.82 E=4. F=6.6
G=2.3

and the kicks are given by

$$\Delta p_x = \xi_x \frac{\partial \varphi}{\partial x} \qquad \text{(B2)}$$
$$\Delta p_z = \xi_z \frac{\partial \varphi}{\partial z}$$

А.Л.Герасимов, Ф.М.Израйлев, Дж.Л.Теннисон,
А.Б.Темных

ДИНАМИКА ВЗАИМОДЕЙСТВИЯ ВСТРЕЧНЫХ ПУЧКОВ

Препринт
№ 86-100

Работа поступила - 19 апреля 1986 г.

Ответственный за выпуск - С.Г.Попов
Подписано к печати 16.06.86г. МН 11758
Формат бумаги 60x90 1/16 Усл.1,5 печ.л., 1,2 учетно-изд.л.
Тираж 200 экз. Бесплатно. Заказ № 100

Ротапринт ИЯФ СО АН СССР, г.Новосибирск, 90